Published in final edited form as:
Langmuir. 2008 September 2; 24(17): 9286–9294. doi:10.1021/la801130w.

High-Resolution NMR Characterization of a Gel-like Surfactant Mesophase

Limin Liu[†], **Grace Tan**[†], **Gary McPherson**[‡,*], **Vijay T. John**[†,*], **Karol Maskos**[§], and **Arijit Bose**[‖]

[†]Department of Chemical and Biomolecular Engineering, Tulane University, New Orleans, Louisiana 70118

[‡]Department of Chemistry, Tulane University, New Orleans, Louisiana 70118

[§]Coordinated Instrumentation Facility, Tulane University, New Orleans, Louisiana 70118

[‖]Department of Chemical Engineering, University of Rhode Island, Kingston, Rhode Island 02881

Abstract

The addition of phosphatidylcholine to AOT water-in-oil microemulsions leads to the formation of a rigid gel as the water content is increased above a specific threshold. This system is a gel-like crystalline phase where the microstructure evolves from reverse hexagonal to lamellar with increasing water content and/or temperature. Couette sheared ^{1}H and ^{31}P NMR experiments carried out at varying temperature and water content show distinct signatures with microstructure evolution. Because the system has been fully characterized through small-angle neutron scattering, it is possible to relate the NMR signatures to the microstructure. The NMR technique therefore complements scattering techniques but is additionally useful because the technique also picks up isotropic signatures from concurrently occurring noncrystalline phases. The use of NMR to identify such lyotropic gel-like crystalline phases allows easy correlation between templated materials synthesis in these phases and phase microstructure. NMR can therefore be used as a probe to understand microstructure in specific surfactant systems and to characterize the retention of microstructure during materials synthesis.

Introduction

Systems that are composed of oil, water, and an amphiphilic surfactant when thoroughly mixed can form thermodynamically stable structures.[1] These microstructures can vary from lamellar layers of oil and water,[2] to well-defined spherical droplets or cylinders of one phase dispersed throughout a bulk phase,[3] intercontiguous networks,[4] or disordered/ordered bicontinuous networks of both phases.[5,6] In all of these microstructures, the surfactants form a stable amphiphilic layer that separates the aqueous and organic phases into well-defined and observable domains.[7]

The current study is directed toward the use of ^{31}P and ^{1}H NMR as easily accessible probes to characterize the microstructure of crystalline surfactant mesophases. While small-angle X-ray and neutron scattering provide significant information about structural characteristics of crystalline surfactant mesophases, these are global techniques that relate to the entire sample.

*Corresponding author. Phone: 504-865-5883. E-mail: vj@tulane.edu.

We demonstrate in this article that similar and complementary information can also be obtained from NMR where the signal is sensitive to the local environment of the ^{31}P and ^{1}H nuclei.

^{31}P nuclear magnetic resonance (NMR) spectroscopy is a nonperturbing probe technique for studying the motion and average orientation of the phosphate group in systems that contain phospholipids.[8] Because the electron shell of the ^{31}P nucleus is not spherically symmetric, its chemical shift is a tensor and depends on the orientation of the phosphorus group relative to the external magnetic field.[9–13] In low-viscosity systems, the phosphorus NMR chemical shifts in all directions are averaged into a symmetrical sharp peak as a result of the rapid molecular rotation. In viscous anisotropic systems, the motions of the lipids are restricted, leading to varying NMR chemical shift anisotropies (CSA) that reflect the local environment and thus the phase characteristics. The ^{31}P NMR technique has been successfully used to characterize the polymorphism of phospholipid systems. [13–16]

The system studied in this article is one where the combination of anionic surfactant AOT (bis (2-ethylhexyl) sodium sulfosuccinate)) and zwitterionic phospholipid lecithin (L-α-phosphatidylcholine) leads to a highly rigid and transparent gel-like mesophase that can solubilize both organic solvent (isooctane) and a significant amount of water at appropriate system compositions.[17] When this binary surfactant mixture is dissolved in a nonpolar solvent (e.g., isooctane), and water is progressively added, the system evolves from a low-viscosity solution to a gel-like state with crystalline order illustrated through small-angle neutron scattering measurements. [18] The system is optically clear, has a high viscosity up to 10^6 Pa• s at low shear rates, and has a relatively high rigidity as characterized by a storage modulus (G') of 10^4 Pa.[19] The microstructure of the mesophase evolves from the reverse hexagonal to the lamellar with either increasing water content or with increasing temperature, as deduced from small-angle neutron scattering.[18,20] Through freeze–fracture direct imaging cryo-transmission electron microscopy, we have shown that the lamellar phase is made up of multilamellar vesicular structures.[21] We have also shown through SANS measurements that such rigid crystalline surfactant mesophases in the reverse hexagonal region can be shear-aligned to create templates for materials synthesis and the structure of the template is reflected in the morphology of the ceramic.[22] Of particular interest in these rigid gel-like systems is the fact that the shear alignment of the hexagonal microstructures can be retained for extended time periods after the cessation of shear, thus allowing the decoupling of materials synthesis from shear application.[19,22] Figure 1 illustrates the relevant transitions from reverse hexagonal to lamellar through changing the water content (W_0) or the temperature.

^{31}P NMR is a very specific and useful method for studying the molecular interactions in the mixed AOT + lecithin mesophase because only a single phosphorus atom of lecithin is present in the entire system.[23] In an earlier paper, we demonstrated that residual phosphorus proton dipolar coupling results in an orientation-sensitive NMR chemical shift anisotropy for the reverse hexagonal phase.[24] We have also observed specific ^{1}H NMR spectral shapes in the water band and solvent band that are responsive to orientational effects.

The objective of this work is to delineate the use of ^{31}P NMR and ^{1}H NMR to follow the evolution of microstructure as water is added to the solution of AOT and lecithin in isooctane. The results illustrate the significant potential of the technique to elucidate the microstructure and are fully complementary to SANS.

Materials and Methods

Materials

Lecithin (95% pure, extracted from soybean, phosphatidylcholine) was purchased from Avanti Polar Lipids Inc. and used without further purification. Bis(2-ethylhexyl) sodium

sulfosuccinate (AOT) was purchased from Sigma. Double distilled water was used. Isooctane (99%+), NMR lock agent deuterium oxide (99.9%), deuterated benzene, deuterium dimethyl sulfoxide (DMSO, 99.9%), and tetramethylsilane (TMS) were purchased from Aldrich.

Preparation of Samples

In this study, the lecithin concentration was set at 0.42 M, and the AOT concentration, at 0.85 M. Typically, the required amounts of lecithin and AOT were mixed with 5 Ml of isooctane in a 20 mL scintillation vial. A clear, transparent 0.42 M lecithin, 0.85 M AOT liquid solution was obtained after 20–30 min of sonication and vortex mixing. Water was added to this solution to the required W_0 value (defined as the molar ratio of water to AOT). Table 1 lists the surfactant compositions used, relating W_0 to the weight fractions of the constituents. The samples were left to equilibrate at room temperature for 2 to 3 days. A 0.42 M lecithinin-isooctane solution was also prepared through sonication and vortex mixing as the reference sample.

All samples were subjected to shear before NMR measurement. Generally, 500 μL of sample was transferred into an 8-cm-long, 5-mm-diameter NMR tube using a 5 mL syringe with a 15 cm long needle (2 mm o.d. and 1.5 mm i.d.). Then a 2.5-mm-wide NMR tube, with DMSO lock agent and TMS reference inside, was inserted into the 5 mm NMR tube slowly and carefully without any relative rotation, making sure that the sample height in the tube was within the coil of the instrument. Suitable caps were used to seal the samples. A Bohlin Visco 88 viscometer was used to shear the samples at a shear rate of 5.38 s^{-1} for 10 min. The inner tube was attached to the spindle of the viscometer and rotated with it while the outer NMR tube was held still. The shear step was conducted outside the NMR spectrometer. After the application of shear, the NMR tube assembly (with inner tube) was transferred to the spectrometer for spectrum acquisition.

Nuclear Magnetic Resonance Spectroscopy

High-resolution NMR measurements were conducted on a Bruker FT-NMR spectrometer equipped with a 11.2 T wide-bore superconducting magnet using tunable wide-band probes with a sample diameter of 5 mm. ^{1}H and ^{31}P NMR spectra were performed with field strengths of 500.13 and 202.42 MHz, respectively, at 25 °C. Typically, 8 scans for ^{1}H and 256 scans for ^{31}P were collected to obtain sufficient signal-to-noise ratios. Samples were capped in coaxial NMR tubes and sealed. All NMR measurements were carried out at 25, 40, and 55 °C. The temperature was controlled by a heated air stream around the NMR tube and measured with a thermocouple placed beneath the tube. Samples run at 25 °C require about 5 min to equilibrate before data acquisition, whereas at the higher temperatures, signal acquisition was carried out after 20 min of equilibration.

Results and Discussion

^{31}P NMR Back ground on Microstructure Characterization

Depending on the local symmetry of the phosphorus nucleus, the magnitude of the chemical shift varies as a function of the molecular orientation relative to an external magnetic field. The orientational dependence of the chemical shift is referred to as the chemical shift anisotropy (CSA). The spectrum consists of a broad line shape with three distinct features—the three principle components, σ_{11}, σ_{22}, and σ_{33}, of the shielding tensor. In low-viscosity liquid like systems, the rapid diffusion averages out the broad anisotropy of the phosphorus spectrum into a very narrow symmetric peak at σ^{C}, with[25]

$$\sigma^{C}=\frac{1}{3}(\sigma_{11}+\sigma_{22}+\sigma_{33}) \quad (1)$$

Phosphorus-containing molecules assembled in isotropic systems such as cubic, rhombic, micellar, or reverse micellar phases show a symmetric ^{31}P resonance at σ^{C}, similar to the resonance characteristics observed for liquid systems. However, for molecules assembled into anisotropic assemblies, chemical shift anisotropy (CSA) is present with a value of

$$\Delta\sigma=\sigma_{11}-\frac{\sigma_{22}+\sigma_{33}}{2}=\sigma_{\|}-\sigma_{\perp} \tag{2}$$

where σ_{11}, σ_{22}, and σ_{33} are chemical shifts along three principal directions. The direction corresponding to chemical shift σ_{11} is defined as the unique axis, and hence σ_{11} is also defined as $\sigma_{\|}$, the chemical shift when the field is parallel to the unique axis. $\sigma_{\perp}$is the chemical shift when the unique axis is perpendicular to the magnetic field and is the average of σ_{22} and σ_{33}.[26]

Phospholipids can assemble into micelles, vesicles, bilayers, and aniosotropic liquid-crystalline phases such as lamellar and hexagonal structures.[27,28] We focus on transformations between the lamellar and hexagonal crystalline microstructures. Figure 2 illustrates the characteristic ^{31}P NMR CSA for these two phases. The characteristic CSA corresponding to the lamellar phase exhibits an upfield peak ($\sigma_{\perp}^{L}$) and a downfield shoulder ($\sigma_{\|}^{L}$), where the unique axis is the symmetric axis of the lipid molecule. When the phospholipids are assembled into a reverse hexagonal phase, the unique axis of the assembly becomes the axis of the cylinder. Because the magnetic field will be roughly normal to the fatty acyl chains along this axis, the value of $\sigma_{\|}^{H}$ is similar to that of $\sigma_{\perp}^{L}$. However, $\sigma_{\perp}^{L}$ will be an average of $\sigma_{\perp}^{L}$ and $\sigma_{\|}^{H}$, owing to rapid motion around the cylinder axis of the entire phospholipid assembly. The corresponding ^{31}P NMR spectrum has the opposite anisotropy, a downfield peak ($\sigma_{\perp}^{H}$) and an upfield shoulder ($\sigma_{\|}^{H}$). The spectral width of the reverse hexagonal phase is half of that of the lamellar phase, as illustrated in the following equations:

$$\sigma_{\|}^{H}=\sigma_{\perp}^{L} \tag{3}$$

$$\sigma_{\perp}^{H}=\frac{1}{2}(\sigma_{\perp}^{L}+\sigma_{\|}^{L}) \tag{4}$$

$$\Delta\sigma^{L}=2\Delta\sigma^{H} \tag{5}$$

The above relationships of the chemical shift anisotropy have been applied to differentiate the hexagonal and lamellar lipid phases in phospholipid systems.[29]

We use this background information together with our earlier results through SANS[18] to characterize phase transitions in the system containing AOT, lecithin, isooctane, and water. There are distinct aspects of this system that make it very interesting to examine. In particular, the system does not show the characteristic reverse hexagonal spectra of Figure 2a because the gel-like phase leads to a nonuniform distribution of crystalline domains. However, when the system is Couette-shear-aligned, the precise NMR signature of the reverse hexagonal phase emerges. These observations are described in detail in our earlier paper.[24] All systems were therefore subjected to Couette shear prior to acquisition of the NMR spectra.

General ^{31}P NMR Characterization

The system compositions investigated in this study are listed in Table 1. The ^{31}P NMR spectrum for the reference sample of 0.85 M lecithin dissolved in isooctane shows the expected symmetrical resonance peak at −0.7 ppm (Figure 3a). A broader resonance peak that shifts downfield to 0.5 ppm is observed when AOT is added to the system at the prescribed concentration of 0.42M(Figure 3b). The downfield shift indicates that the addition of AOT provides a deshielding of the phosphorus nucleus and is evidence that the environment around the phospholipid is changed through the addition of the anionic surfactant.[30] The line broadening also reflects a small decrease in the molecular mobility of the phospholipids, but the high peak symmetry indicates that the lecithin molecules are in small assemblies that have relatively unrestricted mobility. The symmetric peak at around 0 ppm is defined as the isotropic resonance peak.

The intensity of the isotropic peak begins to decrease once water is introduced into the system. Figure 4 illustrates the ^{31}P NMR spectra with W_0 = 10, 30, 50, 70, 90, 110, 130, 150, and 170. The isotropic peak gradually decreases in peak intensity with an increase in water content and totally disappears when W_0 attains 70. At around W_0 = 30, the system exhibits non-Newtonian shear-thinning behavior with a sharp increase in zero shear viscosity around W_0 = 50.[17] By W_0 = 70, the system has a rigid gel-like appearance with a zero shear viscosity as high as 10^6 Pa• s.[19] The NMR data for W_0 = 50—110 exhibits an intense downfield peak at about 4 to 5 ppm with a shallow upfield shoulder at around −11 ppm ($\Delta\sigma$ = 15–16 ppm), a characteristic reverse hexagonal pattern. The data on this mesophase characteristic is fully corroborated by SANS measurements,[18] but it is interesting that the NMR technique is also able to pick up an isotropic region at W_0 = 50. When the water content is further increased to W_0 = 150, the spectrum is reversed in line shape and broadened by a factor of about 2 ($\Delta\sigma$=−24 to −28 ppm), where an upfield peak (~ −11 ppm) is present along with a long downfield tail (~17 ppm). This type of spectrum is typical of a lipid lamellar structure. The spectra recorded at an intermediate W_0 such as 130 shows a superimposed spectral shape from the hexagonal and lamellar patterns, strongly indicating the coexistence of the two microstructures.

The hexagonal pattern and lamellar patterns observed here have similar relationships to those described in eq 3–eq 5. This agreement serves as a good illustration of system microstructure. The observations suggest that a reverse hexagonal structure begins to form at W_0 = 50 and dominates from W_0 = 70–110. At W_0 = 130, the hexagonal structure coexists with the lamellar structure. When the water content is further increased to W_0 = 150 and 170, the lamellar phase dominates. Thus, the NMR experiments reveal a phase transition from reverse hexagonal to lamellar structure with increasing water content in the AOT/lecithin dual surfactant system. This result is in good agreement with our earlier SANS measurements.[18] We note that a broad peak (−0.7 ppm) arises at W_0 = 170, with the same chemical shift as for the isotropic peak. This peak is a consequence of ^{31}P being present in a noncrystalline phase. Our earlier work on cryo-TEM of these phases has deduced that the lamellar phase is a vesicular phase consisting of multilamellar vesicles.[21] The regions between the vesicles therefore contain motionally restricted surfactants in an amorphous state, and these are the signals picked up through NMR. Whereas the lamellar phase dominates the overall spectra, it is evident that NMR is able to pick out resonances from the surfactants that are not in the crystalline phase.

We also examined the phase transitions of this system as a function of temperature. Figures 5 illustrates the ^{31}P NMR spectra for samples with W_0 = 50, 70, 90, 110, 130, 150, and 170 at 40 °C. At water contents of $W_0 \leq 50$ (data shown only for $W_0 \geq 50$), there is an isotropic peak very similar to that in Figure 4 at low water content. Subsequently, the spectral transitions occur as the gel-like mesophase forms. The isotropic peak intensity decreases with increasingW_0 and totally disappears at W_0 = 70. A characteristic hexagonal spectral pattern begins to appear at $W_0 \geq 50$. For rigid gels at W_0 = 70 and 90, the reverse hexagonal spectrum

dominates. The lamellar spectral pattern begins to emerge at W_0 = 110 with an upfield resonance peak (~ −11 ppm) with a shallow downfield shoulder (~16 ppm).Abroad isotropic peak (−1.0 ppm) is also observed together with the lamellar-type spectral pattern at W_0 = 170, which we again attribute to surfactant in the intervening region between the multilamellar vesicles. Similar trends are observed at a higher temperature of 55 °C (Figure 6) with the notable observation that the transition to the lamellar structure occurs at lower W_0 values.

Table 2 summarizes all of the above observations and lists all of the chemical shifts and chemical shift anisotropy values that are observed. σ_s refers to the chemical shift of the shallow shoulder; σ_{p1} is the chemical shift of the primary resonance peak, and σ_{p2} is the chemical shift of the smaller resonance peak. σ_{iso} represents the chemical shift of the isotropic resonance, $\sigma_\perp$ refers to the perpendicular part of the phosphorus chemical shift anisotropy, and $\sigma_\parallel$ refers to the parallel part of the chemical shift anisotropy. $\Delta\sigma^L$ refers to the chemical shift anisotropy of the lamellar phase, and $\Delta\sigma^H$ refers to that of the hexagonal phase. The data in Table 2 clearly show that the H_{II} to L_α phase transition always occurs through a coexistence region when the temperature of the system is increased, in accordance with the Gibbs phase rule.[31] The reversibility of the phase transition is clearly shown by the NMR results labeled as 25r, which define the spectrum obtained by bringing the system back to ambient temperature. All of these observations are in full agreement with SANS, with the notable observation that the NMR technique is also able to pick up the isotropic peaks that indicate the presence of noncrystalline microstructures.

Correlation with ^{1}H NMR Analysis

Proton NMR data were collected together with the ^{31}P NMR experiments. In high-resolution NMR, there are subtle changes in the water and solvent resonances that correlate with the H_{II}–L_α phase transition of the mesophase.

Figure 7 illustrates the proton NMR spectra at ambient temperature for W_0 = 50–170 illustrating clear changes in the chemical shift with microstructure evolution. AtW_0 = 50, sharp isotropic resonances broaden into the two peaks at 4.50 and 4.39 ppm as the reverse hexagonal mesophase becomes evident. At W_0 = 70 when the system is clearly in the reverse hexagonal phase, a downfield peak (4.43 ppm) with an upfield shoulder (4.20 ppm) is present. Further increases in the water content to W_0 = 90 and 110 show a water proton resonance with a spectral characteristics of W_0 = 70 but with an increased shoulder.[22] When the water content is increased to W_0=130, the water band of the proton spectrum shows only a broad single peak at 4.33 ppm, which is downfield of the isotropic resonance at low W_0 values. Upon further increases in the water content to W_0 = 150 and 170, the water proton resonance remains at 4.33 ppm. Because we know that the lamellar structure is that of multilamellar vesicles, the narrower line width of water resonances in the lamellar phase can be attributed to the increased mobility of water molecules in these microstructures compared to that of water in the hexagonal phase.

The proton resonance of the methyl and methylene groups in the solvent band goes through similar transitions. When the water content is W_0 = 50 and the reverse hexagonal phase begins to form, the solvent resonance starts taking on characteristic patterns. Although it is very hard to understand the nuances in the spectra fully, the composite picture revealed by the data at three different temperatures (25, 40, and 55 °C in Figure 7–Figure 9, respectively) reveals the consistent pattern that methyl and methylene solvent resonances in the reverse hexagonal region are distinct from the resonances of the same protons in the lamellar region. The resonances in the lamellar region are sharper and are consistent with the sharpening of the water proton spectra in this region.

In summary, it is clear that in high-resolution ^{1}H NMR subtle but clear distinctions are seen depending on the microstructure. The results are not simply one of line broadening representing

reduced mobility. Indeed, it is observed that there are small changes in the chemical shift indicating that the magnetic fields experienced by the protons in these microstructures are slightly different. In our earlier paper,[24] we showed that the proton resonance characteristics in the reverse hexagonal phase are a function of domain orientation and become consistent only when the domains are aligned through Couette shear. Here, we show variations based on microstructure. In the phase of multilamellar vesicles, the resonances sharpen, showing increased mobility, although they are distinct from the isotropic resonances at low water content.

In summary, a spectral pattern transition was observed for the proton resonance of isooctane's methyl and methylene groups and water molecules with increasing water content. At lower water content, both the solvent and water resonance peaks are sharp, and no orientation effect is observed. For rigid gel samples in the reverse hexagonal region, the orientation effect is reflected in the proton resonance of the methyl and methylene groups and water molecules, where specific chemical shift anisotropies are observed. By further increasing the water content of the lamellar phase, we also observe single resonance peaks for methyl, methylene, and water in the spectrum and the averaging out of chemical shift anisotropies into single resonance peaks.

Similar trends are observed at 40 and 55 °C (Figure 8 and Figure 9). These results are nonintuitive because one would expect both water and solvent molecules to have rotationally averaged out isotropic resonances that are independent of the microstructure. Our explanation is that in these rigid gels made of relatively large assemblies both water and solvent interact strongly with the surfactant and experience subtle changes in field based on the microstructure and orientation of the assemblies.

Conclusions

Our studies indicate that ^{31}P NMR can be used to identify the evolution of crystalline structure in surfactant systems containing the phosphorus nucleus. The technique is fully complementary to scattering in identifying the gel-like crystalline phase, and NMR is also able to identify the presence of isotropic phases together with crystalline phases because the technique samples all environments of the ^{31}P nucleus. ^{1}H NMR of the water and solvent reveals clear signatures relating to the hexagonal crystalline phase that is rather counterintuitive because one would expect an isotropic motion for these species. The sharpening of these resonances as the structure evolves into a multilamellar vesicle phase is indicative of a transition to a more isotropic state.

The NMR technique is therefore a very useful and accessible technique for characterizing microstructure. Such surfactant mesophases have potential uses as vehicles for drug delivery of both hydrophilic and hydrophobic species, especially in formulations for topical applications. They are also useful as emplate materials. The characterization of structure through MR helps us understand the stability of these mesophases hen other components are incorporated into such systems. From another perspective, small amounts of phospholipids may be doped into synthetic surfactant systems exhibiting liquid-crystalline phases without the disruption of the mesophase. ^{31}P NMR may then be used to identify and characterize these mesophases. These studies are in progress.

Acknowledgment

Funding from the National Science Foundation (grant 0438463) and the National Institutes of Health (grant RO1 EB006493-01) is gratefully acknowledged. This article is dedicated to the memory of Karol Maskos.

References

1. Danielsson I, Lindman B. Colloids Surf 1981;3:391–392.

2. Huh C. J. Colloid Interface Sci 1979;71:408–426.
3. Lagues M, Ober R, Taupin C. J. Phys. Lett 1978;39:L487–L491.
4. De Geyer A, Tabony J. Chem. Phys. Lett 1985;113:83–88.
5. Jouffroy J, Levinson P, De Gennes PG. J. Phys. (Paris) 1982;43:1241–1248.
6. Kaler EW, Bennet KE, Davis HT, Scriven LE. J. Chem. Phys 1983;79:5673–5684.
7. Lichterfeld F, Schmeling T, Strey R. J. Phys. Chem 1986;90:5762–5766.
8. Seelig J. Biochim. Biophys. Acta 1978;515:105–140. [PubMed: 356883]
9. Angelico R, Ceglie A, Olsson U, Palazzo G. Langmuir 2000;16:2124–2132.
10. Dennis, EA.; Plückthun, A. Phosphorus-31 NMR, Principles and Applications. Gorenstein, DG., editor. New York: Academic Press; 1984.
11. Thayer AM, Kohler SJ. Biochemistry 1981;20:6831. [PubMed: 7317356]
12. Sjolund M, Lindblom G, Rilfors L, Arvidson G. Biophys. J 1987;52:145. [PubMed: 2822159]
13. Yeagle PL, Sen A. Biochemistry 1986;25:7518. [PubMed: 3801431]
14. Cullis PR, Kruyff BD, Richards RE. Biochim. Biophys. Acta 1979;559:399. [PubMed: 391283]
15. Cullis PR, Kruyff BD, Richards RE. Biochim. Biophys. Acta 1976:426–433.
16. Seelig, Joachim. Biochim. Biophys. Acta 1978;515:105. [PubMed: 356883]
17. Li S, Irvin GC, Simmons B, Rachakonda S, Ramannair P, Banerjee S, John VT, McPherson GL, Zhou W, Bose A. Colloids Surf., A 2000:174–275.
18. Simmons B, Irvin GC, John VT, McPherson GL, Balsara N, Vivek A, Bose A. Langmuir 2002;18:624.
19. Singh M, Agarwal V, De Kee D, Bose A, McPherson G, John V. Langmuir 2004;20:5693. [PubMed: 16459581]
20. Simmons B, Agarwal V, Singh M, McPherson G, John V, Bose A. Langmuir 2003;19:6329.
21. Agarwal V, Bose A, Singh M, McPherson G, John V. Langmuir 2004;20:11. [PubMed: 15744989]
22. Liu L, Singh M, John V, McPherson G, Bose A, Agarwal V. J. Am. Chem. Soc 2004;126:2276. [PubMed: 14982410]
23. Merhring M, Griffin RG, Waugh JS. J. Chem. Phys 1971;55:746.
24. Liu L, John VT, McPherson G, Bose A. Langmuir 2005;21:3795. [PubMed: 15835939]
25. Cullis PR, De Kruijff B. Biochim. Biophys. Acta 1978;507:207. [PubMed: 626732]
26. Smith, ICP.; Ekiel, IH. Phosphorus-31 NMR, Principles and Applications. In: Gorenstein, DG., editor. New York: Academic Press; 1984.
27. Li G, Fudickar W, Skupin M, Klyszcz A, Draeger C, Lauer M, Fuhrhop J-F. Angew. Chem., Int. Ed 2002;41:1828–1852.
28. Oradd G, Lindblom G, Fontell K, Ljusberg-Wahren H. Biophys. J 1995;68:1856. [PubMed: 7612827]
29. Thurmond RL, Lindblom G, Brown M. Biochemistry 1993;32:5394–5410. [PubMed: 8499443]
30. Mackeben S, Muller M, Muller-Goymann CC. Colloids Surf., A 2001;183–185:699–713.
31. Lee JH, Balsara NP, Krishnamoorti R, Jeon HS, Hammouda B. Macromolecules 2001;34:6557–6560.

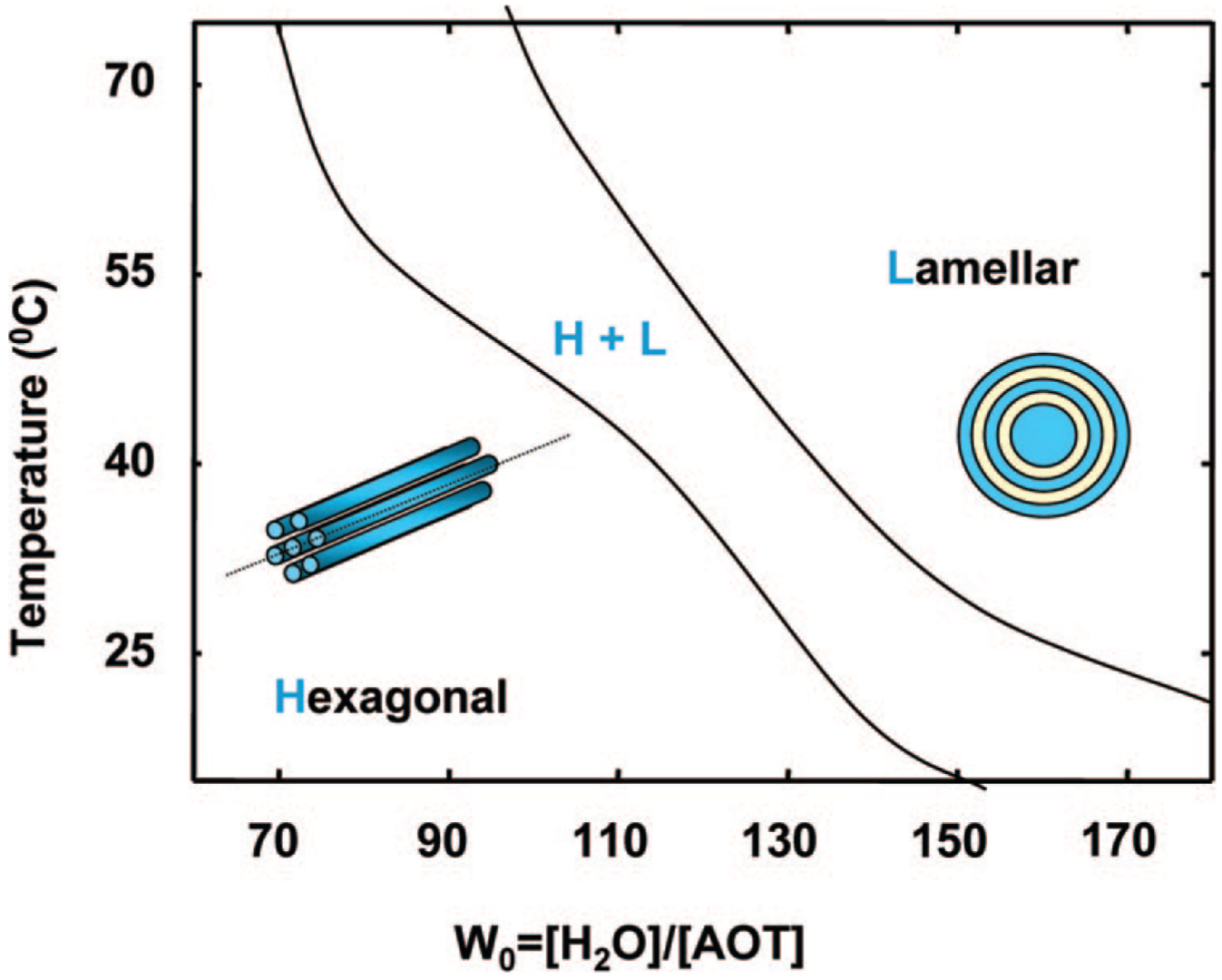

Figure 1.
Phase behavior of the AOT–lecithin system illustrating the transition from the reverse hexagonal (H) to the lamellar (L) phase with increasing water content or temperature. The intervening region exhibits the coexistence of the two phases.

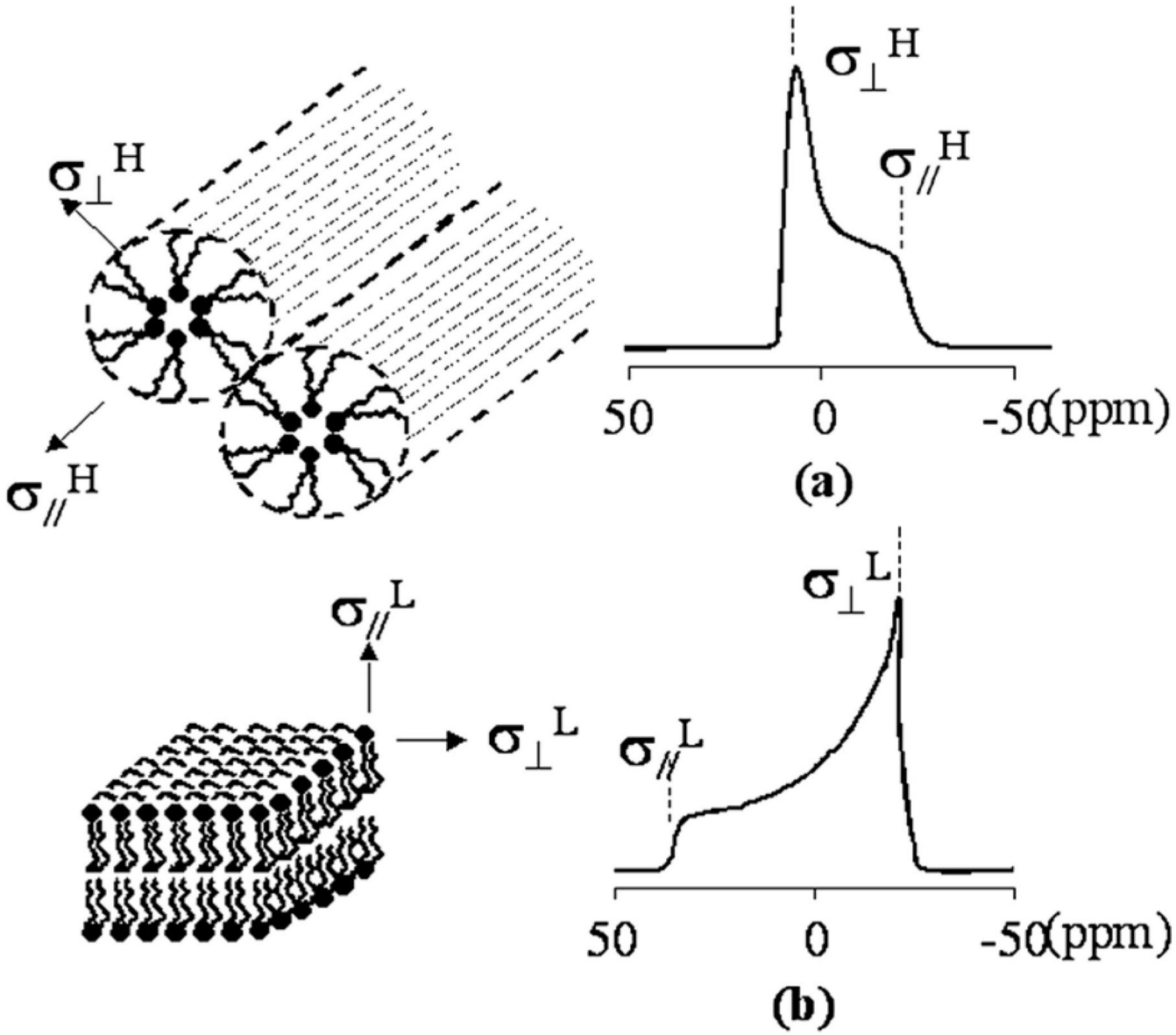

Figure 2.

Representation of the (a) reverse hexagonal phase and (b) lamellar phase formed by lipids and their corresponding ^{31}P NMR spectra. $\sigma_{\perp}$ refers to the chemical shift for the assembly with a unique axis perpendicular to the external magnetic field, and $\sigma_{\parallel}$(parallel component) refers to that for the assembly with the unique axis parallel to the field.

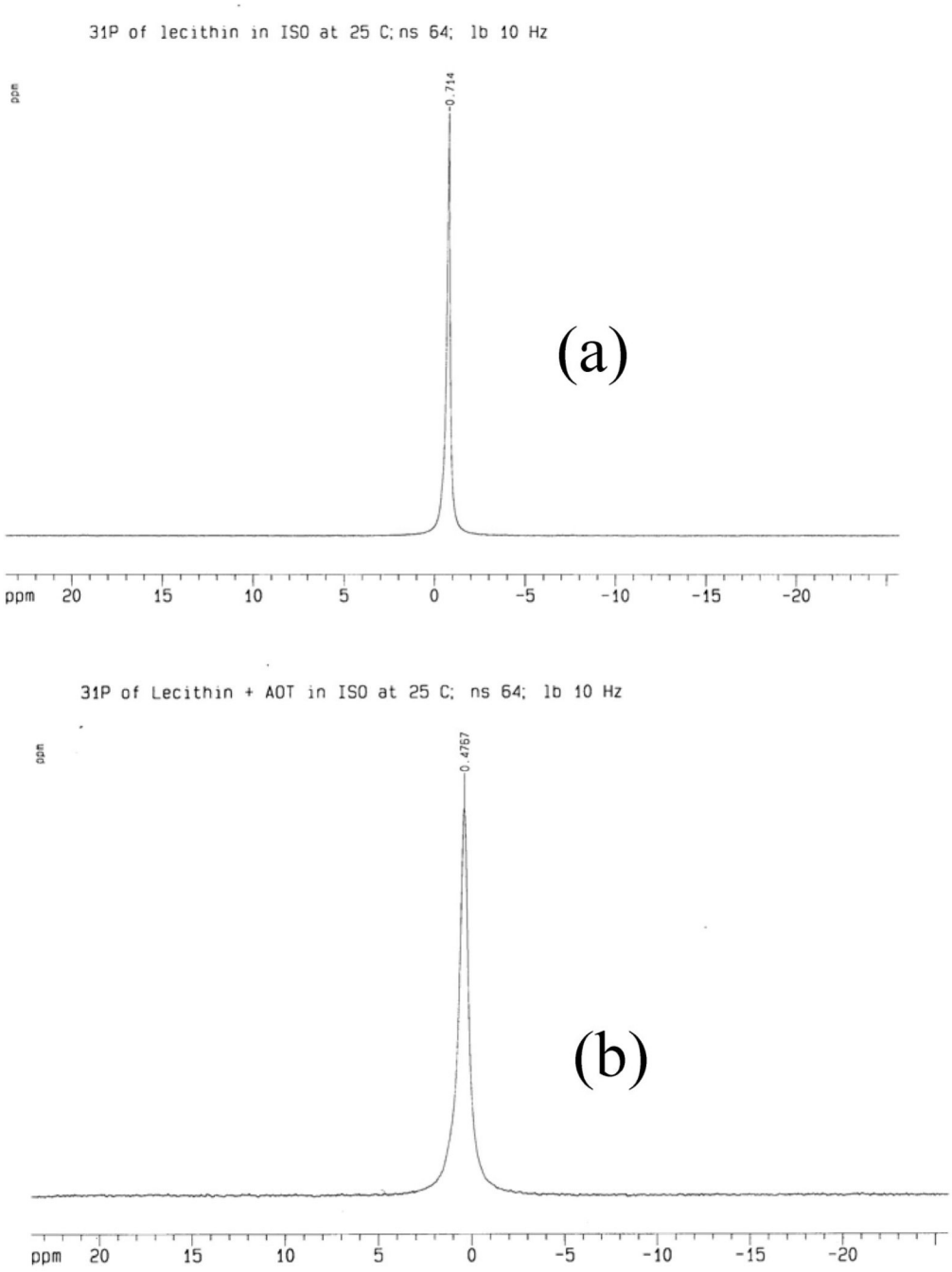

Figure 3.
(a) ^{31}P spectrum of the isooctane solution of lecithin at 25 °C. (b) ^{31}P spectrum of the isooctane solution of lecithin and AOT at 25 °C.

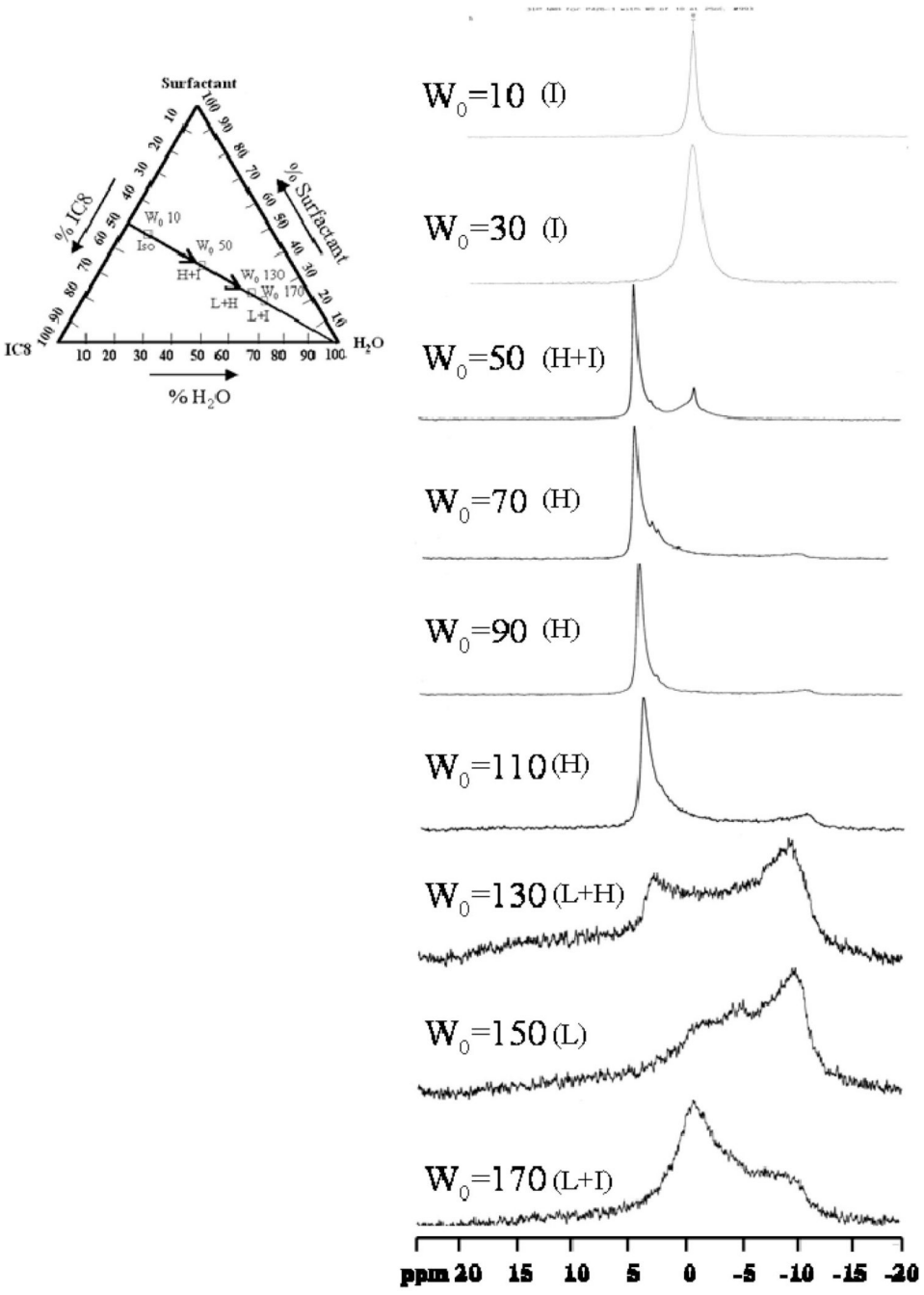

Figure 4.

^{31}P spectra of W_0 = 10, 30, 50, 70, 90, 110, 130, 150, and 170 systems measured at 25 °C. The inset is a ternary phase diagram depicting the sample composition in weight ratio, where I refers to the isotropic phase, H refers to the reverse hexagonal phase, and L refers to the lamellar phase.

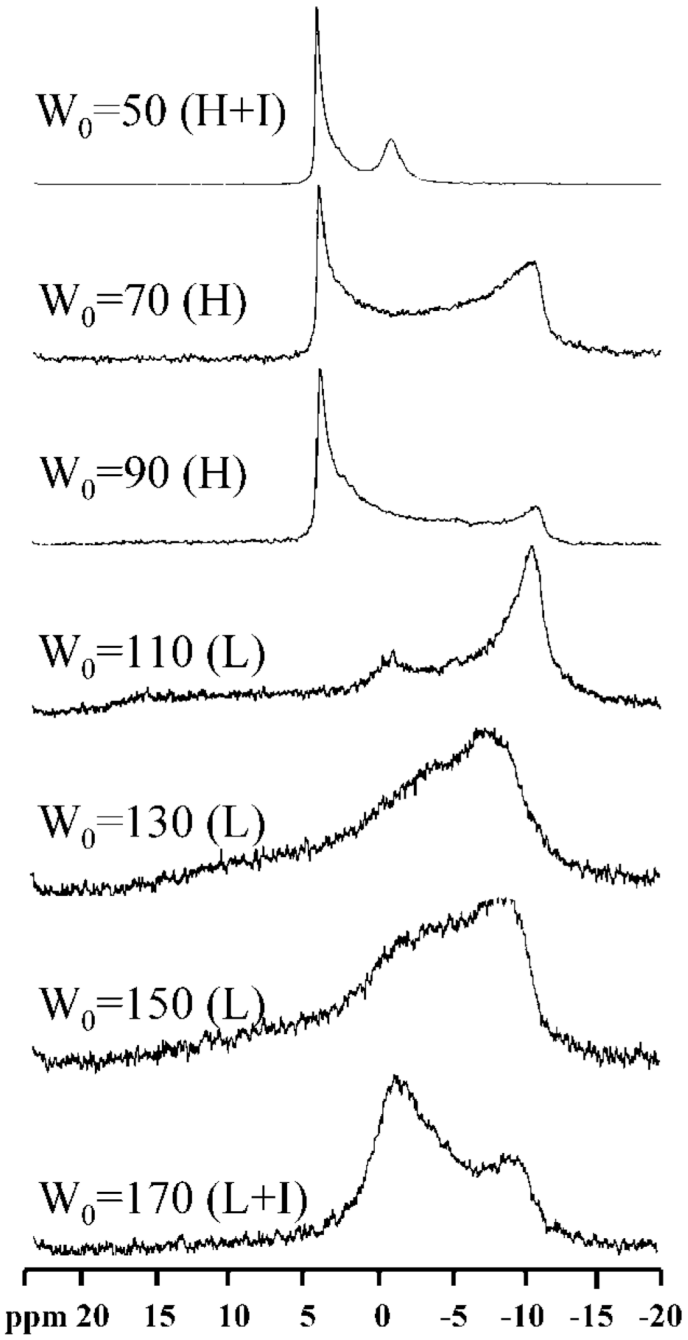

Figure 5.
^{31}P spectra of W_0=50, 70, 90, 110, 130, 150, and 170 systems measured at 40 °C.

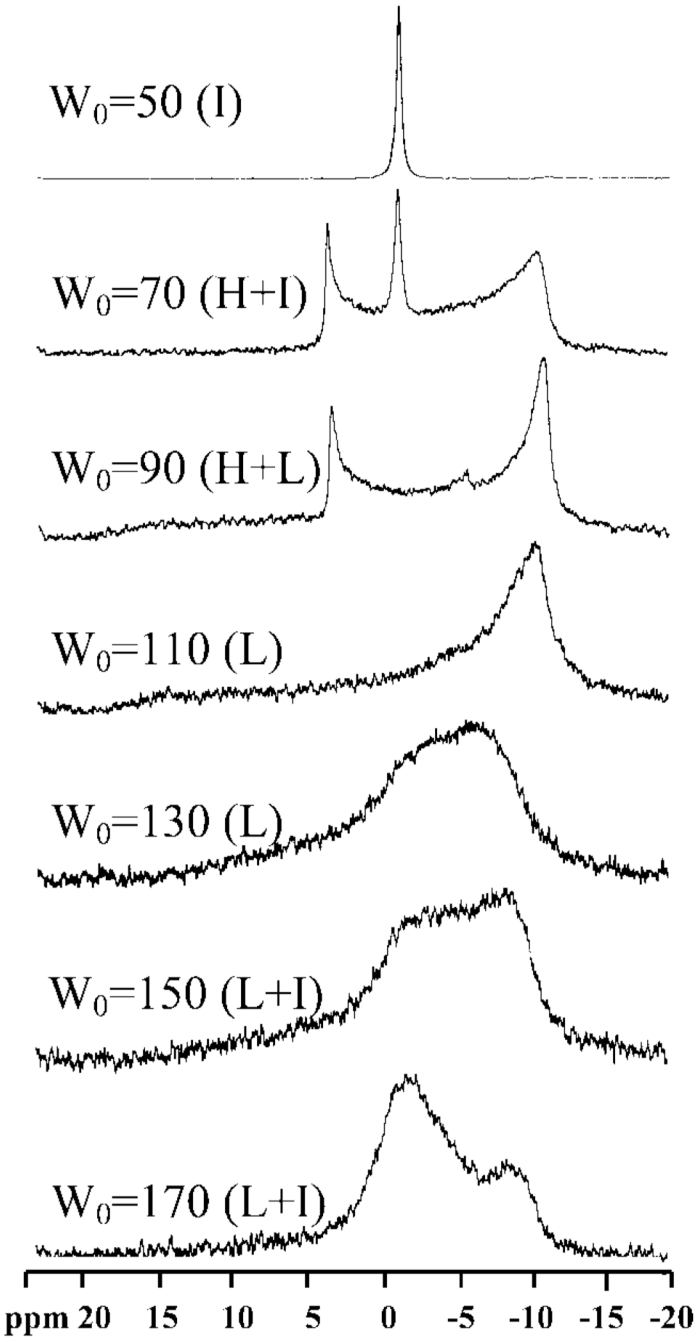

Figure 6.
^{31}P spectra of W_0=50, 70, 90, 110, 130, 150, and 170 systems measured at 55 °C.

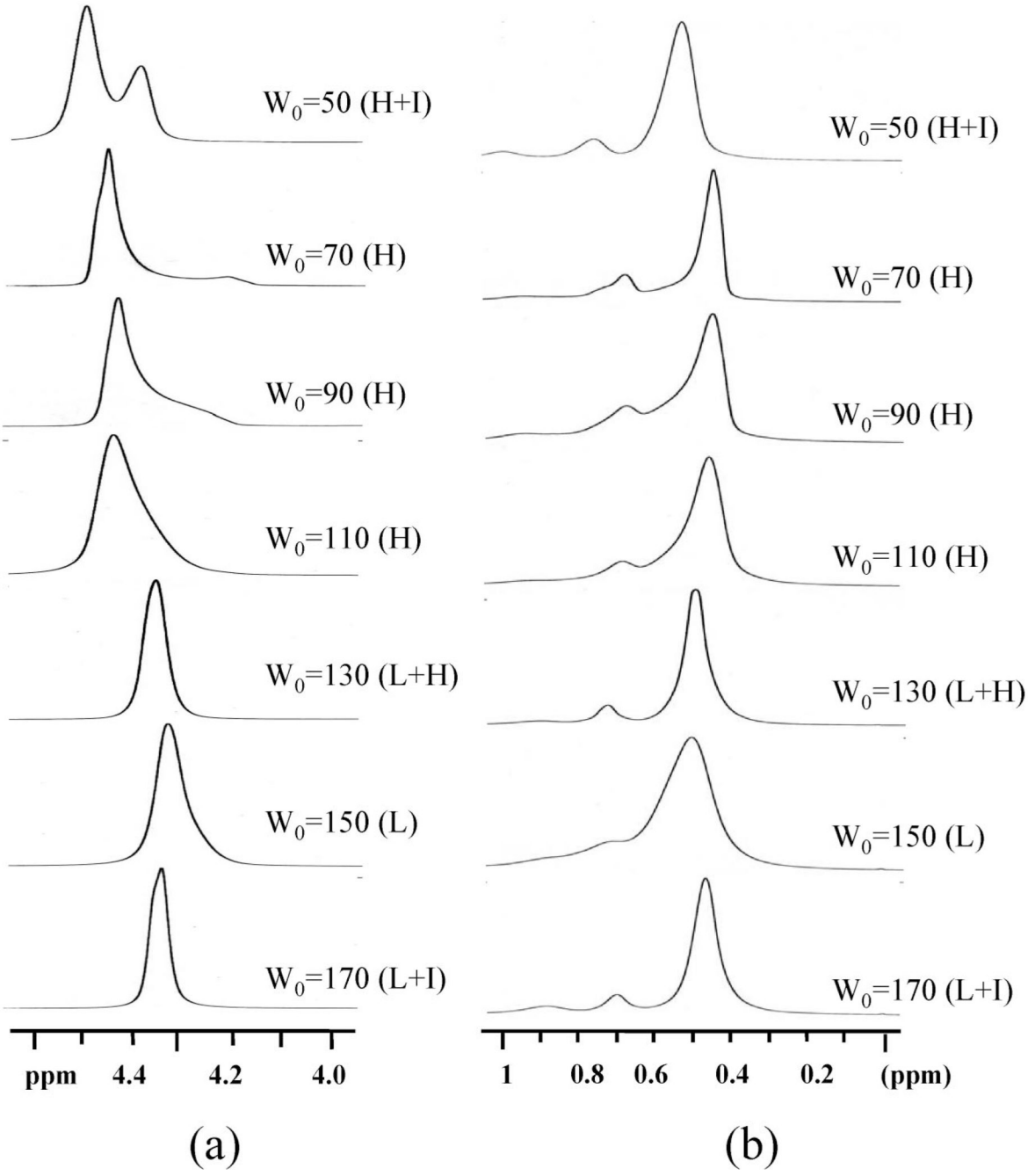

Figure 7.
^{1}H NMR spectra of W_0 = 50, 70, 90, 110, 130, 150, and 170 systems measured at 25 °C.

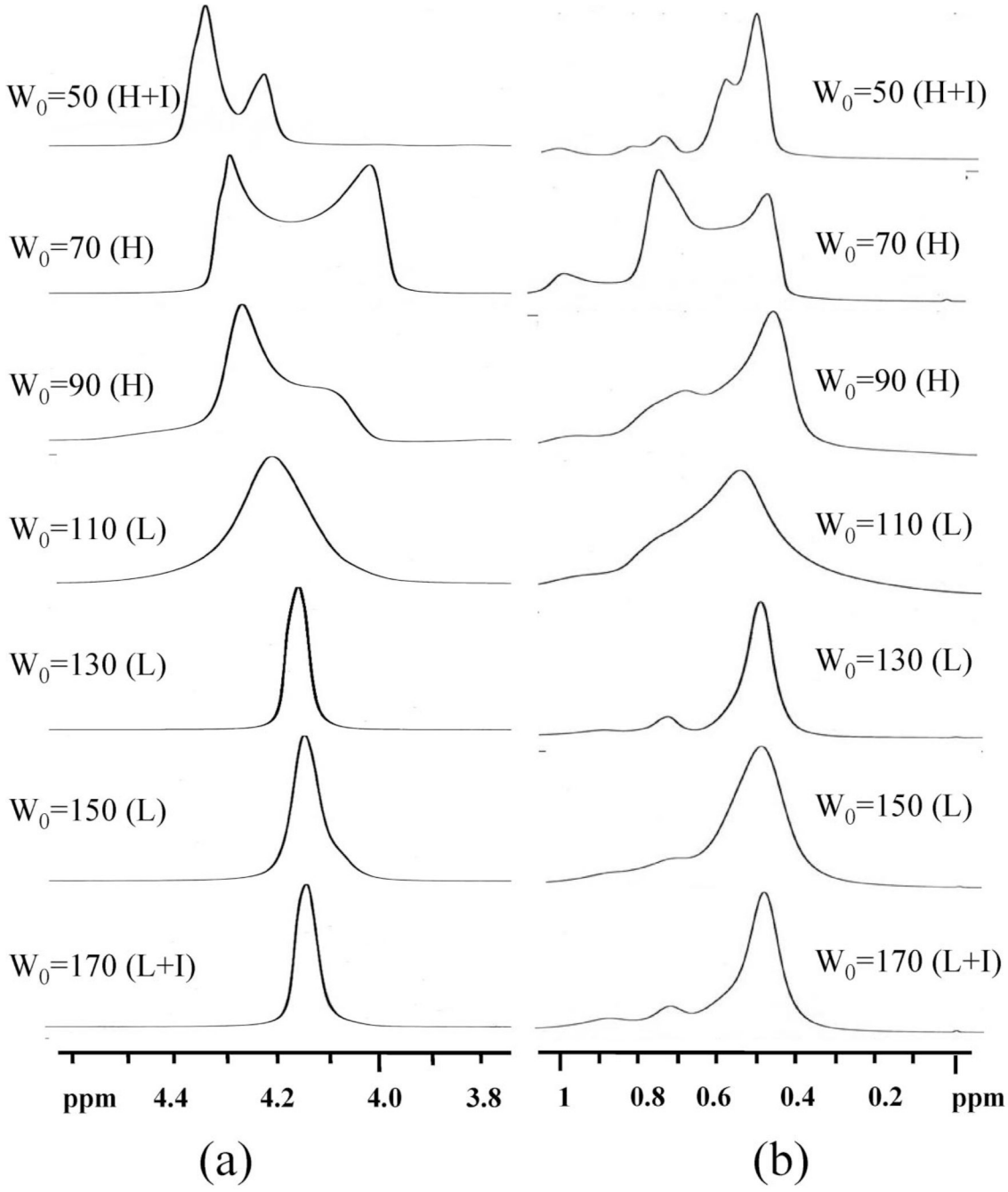

Figure 8.
^{1}H NMR spectra of W_0 = 50, 70, 90, 110, 130, 150, and 170 systems measured at 40 °C.

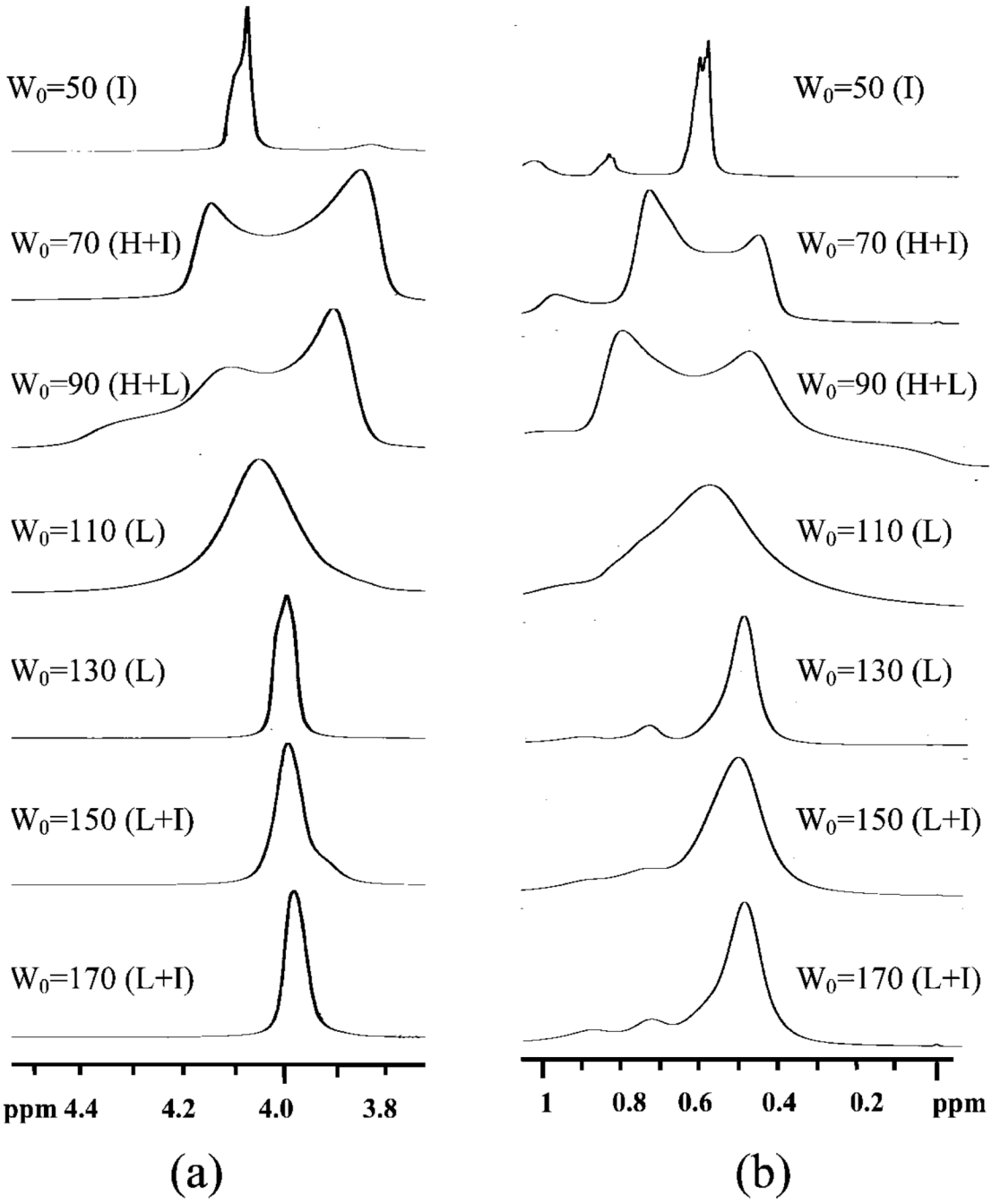

Figure 9.
^{1}H NMR spectra of W_0 = 50, 70, 90, 110, 130, 150, and 170 systems measured at 55 °C.

Table 1

Sample Compositions in the Present Study[a]

W_0	H_2O (g)	α_W	α_S	α_O	Φ_W	Φ_S	Φ_O
0	0	0	0.502	0.495	0	0.240	0.760
10	0.765	0.099	0.452	0.448	0.104	0.215	0.680
30	2.295	0.249	0.377	0.374	0.259	0.178	0.563
50	3.825	0.356	0.323	0.321	0.368	0.152	0.480
70	5.355	0.436	0.283	0.281	0.456	0.131	0.413
90	6.885	0.498	0.252	0.250	0.515	0.118	0.373
110	8.415	0.548	0.227	0.225	0.584	0.106	0.334
130	90945	0.589	0.206	0.204	0.602	0.096	0.302
150	11.475	0.623	0.189	0.187	0.636	0.087	0.276
170	13.005	0.652	0.175	0.173	0.665	0.081	0.255

[a] W_0 is defined as the concentration ratio of water to AOT in the system (W_0 = [H_2O]/[AOT], where 0.85 M AOT (1.89 g) and 0.42 M lecithin (1.59 g) are dissolved in 5 mL of isooctane. α_W, α_S, and α_O denote the weight fractions of the aqueous phase, the surfactant (AOT and lecithin together), and the oil phase, respectively. φ_W, φ_S, and φ_O denote the corresponding volume fractions. In translating experimental weight fractions to volume fractions, an effective surfactant density of 2.2 g/mL was assumed.

Table 2

^{31}P Chemical Shift Values of Samples at Different W_0 Values as a Function of Temperature

W_0	T (°C)	σ_s (ppm)	σ_{p1} (ppm)	σ_{p2} (ppm)	σ_{iso} (ppm)	$\Delta\sigma^H$ (ppm)	$\Delta\sigma^L$ (ppm)	$\sigma_\perp$ (ppm)	$\sigma_\parallel$ (ppm)	phase
50	25	−11.2	4.7		−0.7	15.9		4.7	−11.2	hex + iso
	40	−10.4	4.9		−0.4	15.3		4.9	−10.4	hex + iso
	55				−0.2					iso
	25r	−11.2	4.7		−0.7	15.9		4.7	−11.2	hex + iso
70	25	−10.7	4.3			15.0		4.3	−10.7	hex
	40	−10.8	4.2			15.0		4.2	−10.8	hex
	55	−10.5	4.1		−0.7	14.6		4.1	−10.5	hex + iso
	25r	−10.7	4.3			15.0		4.3	−10.7	hex
90	25	−10.5	4.2			14.7		4.2	−10.5	hex
	40	−10.5	4.2			14.7		4.2	−10.5	hex
	55	16.0	−10.7	4.0		14.7	−26.7			hex + lam
	25r	−10.5	4.2			14.7		4.2	−10.5	hex
110	25	−10.5	4.0			14.5		4.0	−10.5	hex
	40	16.0	−10.8		−0.8	14.8	−26.8			lam
	55	16.0	−10.2				−26.2	−10.2	16.0	lam
	25r	−10.5	4.0			14.5		4.0	−10.5	hex
130	25	19.0	−9.0	4.0		13.0	−28.0			hex + lam
	40	18.0	−9.8				−27.8	−9.8	18.0	lam
	55	19.0	−9.3				−28.3	−9.3	19.0	lam
	25r	17.5	−9.4	4.0		13.4	−26.9			hex + lam
150	25	17.0	−9.5		0		−26.5	−9.5	17.0	lam
	40	15.8	−9.0		0		−24.8	−9.0	15.8	lam
	55	15.0	−9.0		0		−24.0	−9.0	15.0	lam + iso
	25r	16.0	−10.0				−26.0	−10.0	16.0	lam
170	25	15.0	−10.0		−0.7		−25.0	−10.0	15.0	lam + iso
	40	15.0	−10.0		−1.0		−25.0	−10.0	15.0	lam + iso
	55	17.0	−10.0		−1.0		−27.0	−10.0	17.0	lam + iso
	25r	17.0	−9.8		−1.0		−26.8	−9.8	17.0	lam + iso